

Spatial characteristics of AVHRR-NDVI along latitudinal transects in northern Alaska

Jia, Gensuo J.^{1*}; Epstein, Howard E.¹ & Walker, Donald A.²

¹Department of Environmental Sciences, University of Virginia, Charlottesville, VA 22904-4123, USA;

²Institute of Arctic Biology, University of Alaska Fairbanks, Fairbanks, AK 99775-7000, USA;

*Corresponding author: Fax +14349822137; E-mail jjiong@virginia.edu

Abstract. Two-weekly AVHRR images were used to examine spatial patterns of the normalized difference vegetation index (NDVI) and their relationships with environmental variables for moist acidic tundra (MAT) and moist non-acidic tundra (MNT) along two latitudinal transects in northern Alaska. The NDVI database was derived from a 5-yr time series (1995-1999) of two-weekly AVHRR composites for Alaska. A digital climate map, digital elevation map and vegetation map were processed and overlain with the NDVI grid. Homogeneous vegetation patches for both MAT and MNT were defined as sample sites using infrared aerial photos, MSS images and the vegetation map along the transects. Linear and non-linear regression modeling were performed between NDVI indices and environmental variables, total summer warmth (TSW) and elevation. It was demonstrated that along both western and eastern transects, there were obvious latitudinal trends of peak NDVI (AP-NDVI), average growing season NDVI (GS-NDVI), and early June NDVI (EJ-NDVI). In most cases, MNT had lower NDVI values than MAT throughout the year. There were significant ($p < 0.01$) relations between NDVI (AP-NDVI, GS-NDVI and EJ-NDVI) and total summer warmth (TSW) and elevation in the region. EJ-NDVI showed the strongest correlation with TSW or elevation, making it the most sensitive NDVI indicator along environmental gradients in northern Alaska. NDVI was likely controlled by TSW and elevation, with the former being dominant.

Keywords: Arctic; High-latitude; Spatial pattern; Tundra.

Nomenclature: Yurtsev (1994).

Abbreviations: AK = Alaska; AP-NDVI = Annual peak NDVI; AVHRR = Advanced Very High Resolution Radiometer; DEM = Digital elevation model; EJ-NDVI = Early June NDVI; GS-NDVI = Growing season NDVI; LAI = Leaf-area index; MAT = Moist acidic tundra; MNT = Moist non-acidic tundra; NDVI = Normalized difference vegetation index; TSW = Total summer warmth.

Introduction

There is growing consensus that arctic regions will experience marked changes in precipitation, temperature, and the timing of seasonal climate events (Billings et al. 1982, 1997; Bradley et al. 1993). Although the magnitude and direction of these changes are still unclear (Chapin et al. 1996; Oechel et al. 1993, 2000; Shaver et al. 1992), they are likely to affect a wide variety of tundra ecosystem properties (Oechel et al. 1993; Weller et al. 1995; Billings et al. 1997). Arctic vegetation appears to be particularly sensitive to climate changes (Chapin et al. 1995; Arft et al. 1999; Walker et al. 2002, Epstein et al. 2000). An improved understanding of the controls of tundra vegetation patterns across the arctic landscape will be an important input to future climate change studies.

The normalized difference vegetation index (NDVI) has been shown to be a key indicator for the dynamics of vegetation structure and function (Goward et al. 1991; Gutman et al. 1994). Because NDVI is gathered daily and covers large areas, it has been widely used for monitoring spatial gradients and intra-seasonal dynamics of vegetation, especially in large and remote regions such as northern Alaska (Hope et al. 1993; Huete & Jackson 1987; Gutman et al. 1994; McMichael et al. 1997). Walker et al. (1995) even demonstrated a relationship between geological surface age and NDVI in northern Alaska.

Two latitudinal transects, a western transect (West-AK) and an eastern transect (EastAK), are being used by the Arctic research community to examine spatial patterns of biophysical features along latitudinal gradients in northern Alaska (Anon. 1997; Weller et al. 1995). Several studies were conducted that examined the biophysical controls of spectral reflectance on the eastern transect (Stow et al. 1993; Shippert et al. 1995; Walker et al. 1995; McMichael et al. 1997). One of the studies produced biomass and leaf-area index (LAI) maps of the

Toolik Lake region derived from SPOT satellite data (Shippert et al. 1995). Another showed a linear correlation between NDVI and landscape age on three glacial surfaces spanning ca. 125 000 yr (Walker et al. 1995). McMichael et al. (1999) demonstrated a relationship between NDVI and measurements of mean site gross photosynthesis and ecosystem respiration at two sites in Arctic tundra ecosystems in the Toolik Lake area.

Previously, most of the Foothills region in northern Alaska, and the Low Arctic in general, was assumed to be moist acidic tundra (MAT), or typical tussock tundra (Shaver & Chapin 1991; Oechel et al. 1993). Since the description of MNT in the 1990s (Walker et al. 1994, 1998) researches have focused on comparison of ecosystem properties of the two types and on the boundaries between them (Walker et al. 1998; Bockheim et al. 1998; Muller et al. 1999). However, there has been no research conducted on the spatial gradients of vegetation or spectral features for MAT and MNT in northern Alaska.

There are many differences between MAT and MNT. In MNT, the dominant plant association is *Dryado integrifoliae-Caricetum bigelowii*. Dominant plant species include *Carex bigelowii*, *Eriophorum triste*, *Dryas integrifolia*, *Salix reticulata*, *S. lanata*, *Lupinus arcticus*, *Astragalus umbellatus*, *Tomenthypnum nitens*, *Ditrichum flexicaule*, *D. capillaceum* and *Thamnolia subuliformis*. The dominant life form is tussock graminoid (Walker et al. 1994). The pH of the top mineral horizon is > 6.5. In MAT, the dominant association is *Sphagno-Eriophoretum vaginati*. The dominant plant species are *Eriophorum vaginatum*, *Betula nana*, *Ledum palustre* ssp. *decumbens*, *Salix planifolia* ssp. *pulchra*, *Rubus chamaemorus*, *Aulacomium turgidum* and *Sphagnum girgensohnii*. The dominant life form is dwarf shrub (Hansen 1953; Walker et al. 1994), and the pH of the top mineral horizon is < 5.5. A recent study also indicated important differences in numerous ecosystem properties between MNT and MAT, such as gross primary production (1820 mg CO₂-C m⁻² d⁻¹ in MAT compared to 940 in MNT), leaf area index (0.84 m² m⁻² in MAT compared to 0.50 in MNT), and bare soil coverage (0.8% in MAT compared to 7.5% in MNT) (Walker et al. 1998). We assume that there should be a major difference in NDVI between the tundra types corresponding to their difference in ecosystem structure and functions.

The objective of this paper is to investigate remotely the spatial patterns in vegetation along latitudinal transects in northern Alaska. The questions we address here are: 1. What is the spatial distribution of NDVI across the North Slope of Alaska? 2. What controls the spatial patterns of NDVI in the study area?

Methods

Study sites

The North Slope of Alaska, north of the Brooks Mountain Range, beyond the Arctic Circle, is dominated by tundra vegetation. From north to south, there are three major eco-regions: the coastal tundra (0 - 50 m elevation), the foothills tundra (50 - 700 m), and the Brooks Mountain Range (> 700 m) (Fig. 1a). Two arctic transects have been established as part of the NSF Land-Atmosphere-Ice Interactions program to conduct integrated tundra research (Weller et al. 1995; Walker et al. 1998). The western transect starts at Barrow, the northern tip of the state, and runs through Atkasuk and Oumalik to Ivotuk; the eastern transect, starts at Prudhoe Bay on the coast, and ends at Toolik Lake, a Long-Term Ecological Research (LTER) site. Our remote sensing studies are conducted along these two transects (Fig. 1a).

Processing of AVHRR-Derived NDVI

The Normalized Difference Vegetation Index (NDVI) derived from AVHRR imagery (Markon et al. 1995; Goward et al. 1991) is an index of vegetation greenness: $NDVI = (NIR - R) / (NIR + R)$, where NIR is the spectral reflectance in the near-infrared band (0.725 - 1.1 mm), dominated by light scattering from the canopies, and R is the reflectance in the red chlorophyll-absorbing portion of the spectrum (0.58 - 0.68 mm). For most biophysical research of the earth's surface, cloud-free data are needed. However, daily cloud free data are normally not available, especially in the arctic. Therefore, a series of images is often collected over a set time period (14 d in our data set), with those images containing the least cloud cover being used in a compositing process (Holben 1986; Gutman et al. 1994). The make-up of AVHRR scenes used during the composite period was based on the maximum NDVI value within any particular scene.

1995-1999 AVHRR-NDVI time series data from the EROS Data Center of the USGS were used as basic data sets. The original data were converted into raster GRID format, using Arc/Info, for further spatial analysis. The subset of northern Alaska was taken from the state-wide data, so that only the arctic portion was used in the analysis. The 1995-1999 data sets are based on a 14-day composite period to match the processing of global data sets currently being produced. Data acquisition for each of the five temporal data sets was initiated on April 1 of each year. At this time, over 90% of the state is snow-covered. The ending date was on October 31 when the growing season is over, and snow starts to cover most of the high latitudes (Holben 1986; Markon 1999).

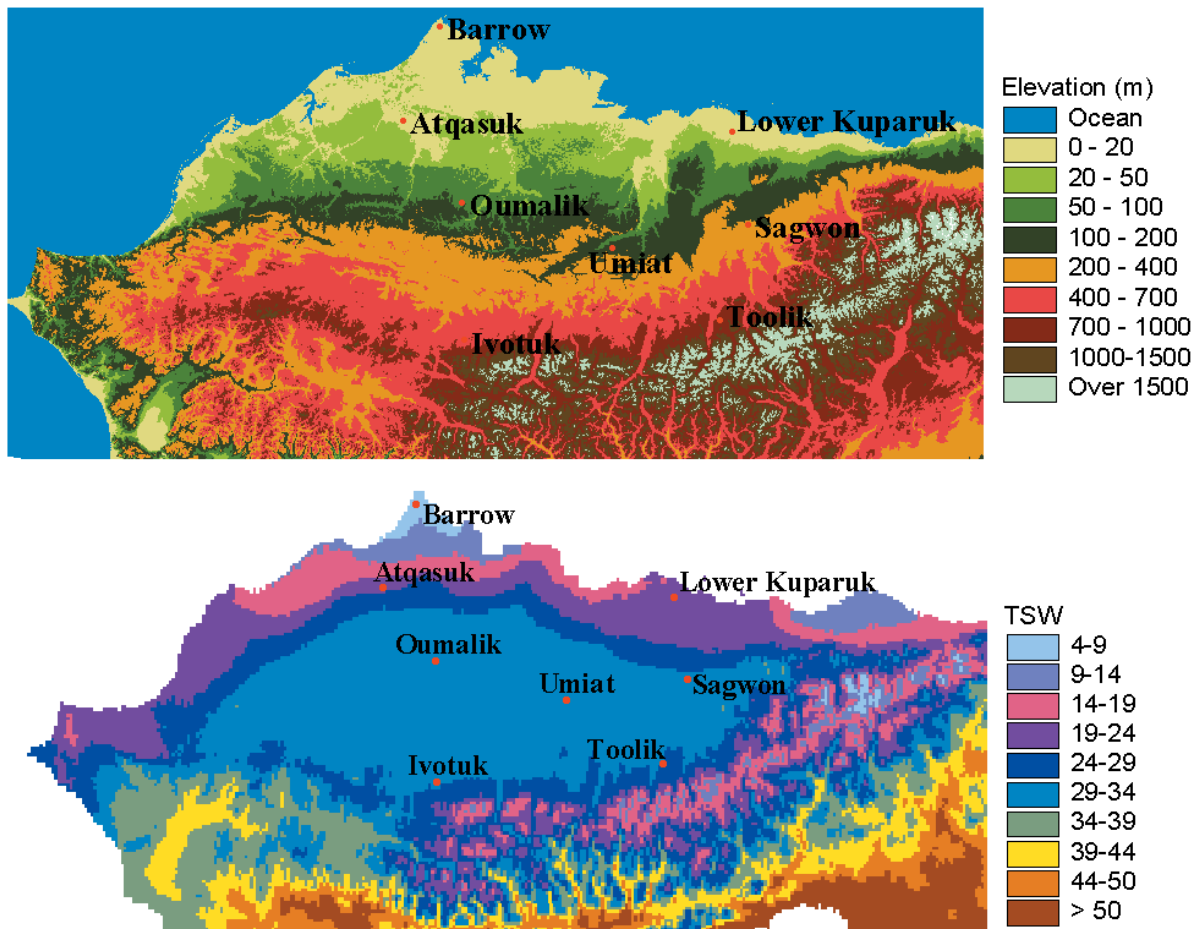


Fig. 1. a. Digital Elevation Model (DEM) for northern Alaska. DEM was processed from the GTOPO30 data set developed by the USGS EROS Data Center. The horizontal grid spacing is 30 arc-sec (or ca. 1 km), while the vertical units represent elevation in meters above sea level, with 1-m resolution. Red points represent the sample sites of field and aerial photo data along both transects (in color). **b.** Total Summer Warmth in northern Alaska, calculated from PRISM monthly mean air temperature spatial surfaces (in colour).

Because it has been shown that cloud contamination persists in two-weekly composites (Gutman et al. 1994), the initial two-weekly composite time series were filtered using the BISE (Best Index Slope Extraction) adaptive filter (Viovy et al. 2000). This filter determines NDVI time series data that are contaminated by cloud cover based on some properties of the temporal signal of NDVI. In particular, it assumes that a decrease of NDVI due to surface change cannot be immediately followed by an increase of NDVI because vegetation cannot regrow over a few weeks. Each period throughout the time series was checked for cloud contamination and growing season snow. Any pixel with less than a 0.09 NDVI value within the growing season was considered as contaminated, and was marked and replaced with an inter-annual mean value (Markon et al. 1995). The advantage of such a method is that it allows retention of the initial time step (and the rapid increase or decrease

of NDVI at the beginning or end of the cycle) and eliminates cloudy events during several months. The filter is also designed to eliminate registration errors that can induce short NDVI high peaks that are then kept by the compositing process.

From the improved NDVI data set, three major NDVI indices were calculated during the 1995-1999 period: annual peak NDVI, growing season NDVI and early June NDVI. Average values from the five-year time series were calculated for these three indices to represent the mean greenness during the late 1990s.

Annual peak NDVI (AP-NDVI) is the maximum measurable NDVI recorded during the year and is normally associated with the peak of green during the growing season (Fig. 2a). Annual peak NDVI for each year was calculated based on the pixel-by-pixel grid model:

$$AP-NDVI = \text{MAX} (\text{period } 1, 2, \dots, n) \quad (1)$$

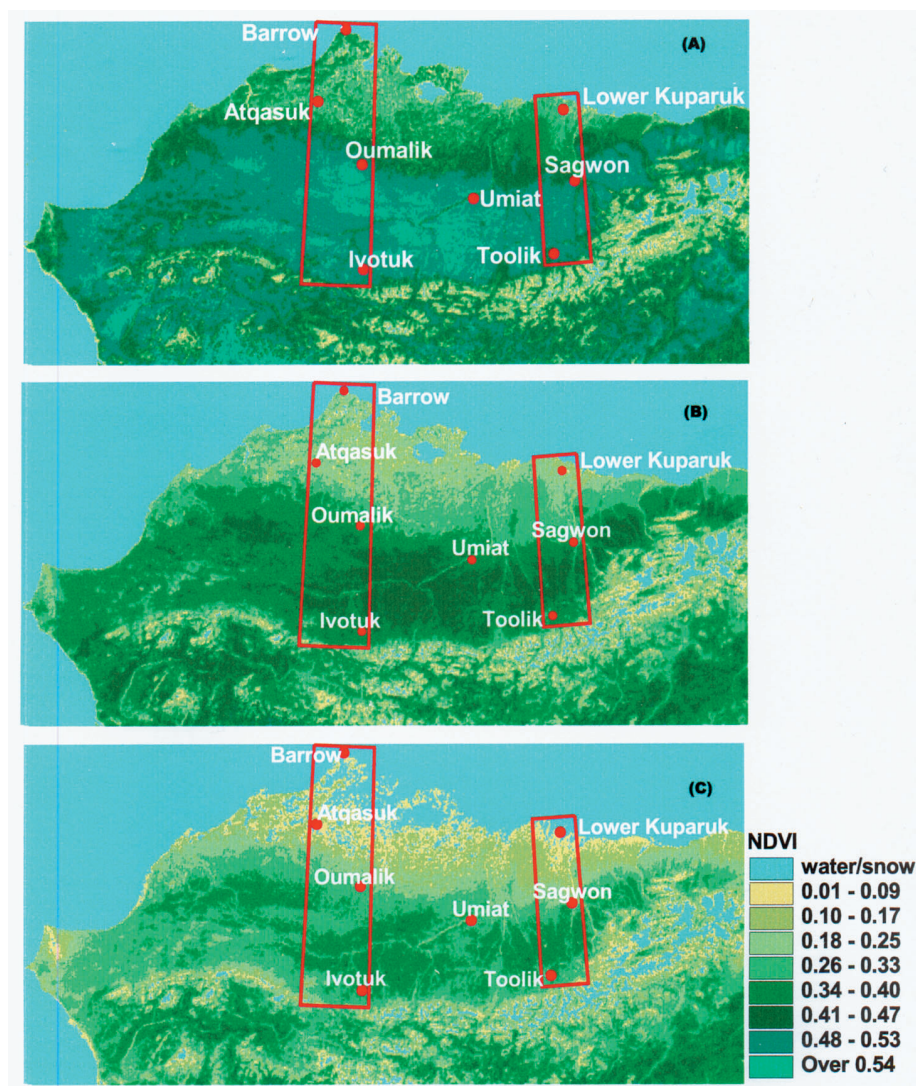


Fig. 2. Maps of NDVI in northern Alaska, calculated from 1995-1999 mean values. **A.** Annual peak NDVI; **B.** Growing Season NDVI; **C.** Early June NDVI. Red polygons represent the spatial extension of both transects.

Average NDVI for the growing season (GS-NDVI) is the average NDVI value obtained across recording periods during the growing season. In most of northern Alaska, the growing season lasts from June to September, so the NDVI two-weekly periods 5 (starts on May 27) to 13 (ends on September 29) were chosen to represent the values during the growing season (Fig. 2b). GS-NDVI was calculated based on the pixel-by-pixel grid model:

$$\text{GS-NDVI} = \text{MEAN}(\text{period } 1, 2, \dots, n) \quad (2)$$

Early June NDVI (EJ-NDVI) is the average values at period 5, from May 27 to June 9. Onset of greenness occurs in most of northern Alaska by early June, and this period is considered as one of the most sensitive to environmental changes (Markon 1999; Hope et al. 1995). Early June NDVI (EJ-NDVI) from 1995-1999 was calculated on a pixel-by-pixel basis (Fig. 2c).

MAT/MNT homogeneous vegetation samples

For the purpose of this study, we were interested in not only environmental controls on tundra types, but also in greenness and productivity within certain tundra types. Therefore we needed to define sample sites for homogeneous tundra types on high-resolution images such as aerial photos and MSS with ground control points. For this approach we picked as many sample sites as possible to represent the study region.

MAT and MNT are widely distributed on the North Slope. Combined they cover more than 60% of the area (Muller et al. 1999). Based on ground-truthing and image interpretation in 1998 and 1999, we marked 91 homogeneous vegetation patches of MAT and MNT on 14 scenes of infrared aerial photos taken along both the western and eastern transect. These aerial photos were then digitized and geo-registered with Arc/Info software.

The control points (in total 127) for the registrations were picked up from 1 : 63 360 USGS topography maps. From the geo-registered aerial photos, the 91 polygons of MAT and MNT were digitized and a scattered vegetation map of MAT and MNT on the transects was created. A comparison analysis between our vegetation map and a MSS derived land cover map (Muller et al. 1999) shows a high agreement (88.9%) between the two. This is the most critical step for our analysis in this study, so we made every effort to gain a high accuracy of the vegetation patches.

Total Summer Warmth (TSW)

Total summer warmth is considered an important indicator of growing season condition (Walker et al. 1998). It is the sum of monthly air-temperatures > 0 °C. TSW was calculated from PRISM monthly temperature GRID data, which was simulated from monthly field air temperature data (Fig. 1a). PRISM climate data are created and provided by the NOAA data center at Oregon State University; they were derived from point data (from ground meteorological stations) and some spatial data sets (distance from coast, elevation, etc), and include estimates of annual, monthly and event-based climatic elements that are gridded and GIS-compatible. The strong variation of climate with distance from coast and elevation is the main premise underlying the PRISM model formulation in northern Alaska (Haugen & Brown 1980; Walker et al. 2002).

In northern Alaska, originally only five meteorological stations were used in the modeling. To verify PRISM accuracy in our study area, we used measurements from 14 locations throughout the North Slope to calculate the correlation between field measurements of temperature and the PRISM grid values, point-by-point, and month-by-month. For all 14 points, the *r*-value > 0.99; for a monthly comparison from March to November, the *r*-value > 0.90. The correlation is lower at Atqasuk and Oumalik, which reflect incomplete field measurements. The PRISM air temperature model is also supported by the study from Haugen & Brown (1980). The accuracy assessment shows that in northern Alaska, PRISM data are valid as a representation of the spatial distribution of monthly temperature; therefore we used PRISM-derived data in our analysis. Throughout northern Alaska, 91 points were derived from PRISM in correspondence with our MAT/MNT vegetation polygons.

Processing a digital elevation model

A GTOPO30 digital elevation model (DEM) was processed and used as one of the basic data sets (Fig. 1).

The GTOPO30 data set, completed in 1996, was developed by the USGS EROS Data Center. The horizontal grid spacing is 30 arc-seconds (or ca. 1 km), while the vertical units represent elevation in meters above sea level, with 1-m resolution. Original image data (in Band Interleaved by Line, BIL, format) were converted to GRID raster data, and several formulas were applied to recognize negative values and adjust the data.

Correlation analysis and regression modeling on controlling factors of NDVI

Corresponding to the 91 sample sites derived from infrared aerial photos, grid values from raster data of NDVI indices, air temperature and geographic features such as elevation and slope were extracted for each polygon and formed the basic data set; there were 27 variables in the original data set. A factor analysis was performed to group the 27 variables and to find out their correlations. Based on the results of the factor analysis, three indices of NDVI (annual peak NDVI, growing season mean NDVI and early June NDVI) and two environmental factors (TSW and elevation) were selected for factor analysis (Table 1). These selected variables were then used to perform correlation analyses with three approaches: (1) combining all the samples sites; (2) categorizing vegetation types as MAT and MNT; (3) splitting samples into two transects. For all the 91 sample sites on the North Slope, regression analyses were performed between: (1) AP-NDVI vs. TSW and elevation; (2) GS-NDVI vs. TSW and elevation; (3) EJ-NDVI vs. TSW and elevation. SPSS software was used for the statistical analyses.

Table 1. Pearson correlation coefficients for selected variables. Calculations were performed for all samples, MAT samples and MNT samples respectively. Only selected variables with the highest correlations were shown here.

Variable	EJ-NDVI	AP-NDVI	GS-NDVI	TSW	Elevation
<i>All samples (N = 91)</i>					
EJ-NDVI	1.000				
AP-NDVI	0.850	1.000			
GS-NDVI	0.947	0.951	1.000		
TSW	0.783	0.560	0.717	1.000	
Elevation	0.727	0.566	0.612	0.439	1.000
<i>MAT samples (N = 48)</i>					
EJ-NDVI	1.000				
AP-NDVI	0.839	1.000			
GS-NDVI	0.959	0.940	1.000		
TSW	0.856	0.630	0.807	1.000	
Elevation	0.763	0.603	0.668	0.502	1.000
<i>MNT samples (N = 43)</i>					
EJ-NDVI	1.000				
AP-NDVI	0.867	1.000			
GS-NDVI	0.915	0.968	1.000		
TSW	0.922	0.854	0.893	1.000	
Elevation	0.633	0.484	0.473	0.424	1.000

Results

Spatial patterns of NDVI along the two transects

In early June, vegetation in most of northern Alaska entered the growing season. Along both transects, NDVI values increased gradually from north to south, following the latitudinal gradient (Fig. 2c). This partly reflected the phenology of different plant functional types (Markon et al. 1995; Vierling et al. 1997). In northern Alaska, the growing season started earlier with decreasing latitude as temperatures rise and moisture availability increase. Consequently, biomass and leaf area index, which were demonstrated to be major contributors of NDVI (Hope et al. 1993; Riedel et al. in prep.), could be expected to follow a similar latitudinal trend in early June. This result was supported by Vierling et al. (1997), who demonstrated that the strongest differences in arctic tundra vegetation types could be found in the early growing season. Along both transects, growing season average NDVI more or less followed the latitudinal gradient, i.e., lower values in the north and higher in the south (Fig. 2b); NDVI reached its peak along the foothills and dropped sharply to the north and slightly to the south where higher elevation causes shorter growing seasons and reduced plant cover.

The images of peak NDVI calculated from AVHRR-NDVI time series showed trends in 'greenness' across both transects that were expected on the basis of geobotanical and land cover maps of the area (Walker 1999; Muller et al. 1999). Water tracks and south-facing slopes, both of which have dense shrub vegetation, showed NDVI values greater than 0.52. Most barren hilltops and water bodies showed NDVI values from 0 to 0.08. Coastal wetlands showed NDVI values between 0.10 and 0.16. These values were consistent with values

reported in literature for the same region (Hope 1994; Markon et al. 1995).

We calculated the average values of peak NDVI with 0.2° intervals of latitude, along both eastern and western transects. In the process, large water bodies were excluded so that only vegetation dominated areas were considered. Both transects start around 68.5° in the south, but the western transect extends further north (71.3°) compared to the eastern one (70.2°). Along the eastern transect, peak NDVI increased slightly northward from the most southern point, and reached its peak around 69°. Then the value dropped sharply from 0.53 to 0.28 on the coastal plain. Along the western transect, peak NDVI remained as high as 0.53 from Ivotuk to 69.2°, then started to drop sharply northward until 70.2° (0.29); it continued to drop slightly to 0.23 at Barrow (Fig. 3). On both transects, peak NDVI more or less followed the north-south gradients, and followed the same trend, but the slight drop in NDVI at their southern ends may reflect the combined influence of latitude and elevation. In the east, there are greater topographic changes than in the west.

Fig. 3 does not necessarily reflect the NDVI gradient of pure zonal vegetation (moist tundra), considering the fact that the moist pixels were becoming more and more mixed with wet vegetation as we move toward the coast. In the foothills the pixels were fairly unmixed, but as we moved onto the coastal plain, there was more and more mixing that cannot be avoided at such a scale. In the western transect, once the wet coastal tundra was reached, the NDVI leveled off at about 0.27-0.24. This analysis therefore integrated changes in elevation, site moisture, and temperature, which were all varying in the same direction geographically, and cannot be teased apart easily along 0.2° latitude intervals.

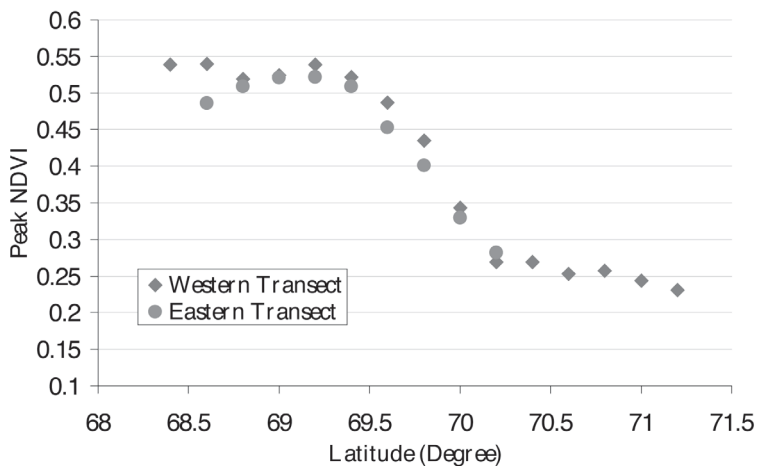


Fig. 3. Latitudinal gradient of peak NDVI along both transects, with 0.2 degree interval of latitude. The NDVI value for each 0.2-degree patch was derived from the average values of all pixels within the patch. The round circle represents the western transect, while the diamond is for the eastern transect.

The bivariate correlation analysis

An initial screening of the data was done to obtain an idea of the level of correlation within NDVI indices as well as the interrelationships between NDVI indices and environmental variables along the transects. In order to examine the potential controlling factors and pick up the most representative ones for further analysis, we started with the 91 samples from both transects as a whole data set and analysed the correlation between NDVI indices (AP-NDVI, GS-NDVI, EJ-NDVI) and a set of environmental factors, including monthly air temperature, annual mean temperature, total summer warmth, monthly precipitation, annual precipitation, elevation and slope. Based on the correlation, two factors, TSW and elevation, were selected for further analysis (Table 1).

A consistently high correlation was found between EJ-NDVI and the two environmental variables (TSW and elevation), though the correlation coefficients and the rankings varied. The correlations between GS-NDVI and the two variables were lower than that for EJ-NDVI, but they were still relatively high ($r=0.717$, $r=0.612$, respectively) and significant ($p<0.01$). It is interesting to notice that as a widely used NDVI index, AP-NDVI

had the lowest correlation with both variables, though still significant ($p<0.01$). The best correlation is found between EJ-NDVI and TSW ($r=0.783$), followed by the one between EJ-NDVI and elevation. While not shown in table 1, precipitation was highly positively correlated with elevation ($r=0.868$), but had a lower positive correlation with all three NDVI indices than elevation. We therefore decided to use elevation instead of precipitation for later regressions.

We calculated more detailed correlations by categorizing vegetation types as MAT and MNT. For all of the treatments it was still found that EJ-NDVI was better correlated to total summer warmth and elevation than GS-NDVI or AP-NDVI. EJ-NDVI was strongly correlated to TSW ($r=0.856$ for MAT and 0.922 for MNT). This was followed by elevation ($r=0.763$ for MAT and 0.633 for MNT) when data were grouped into plant community categories. The results also suggest that the spatial variation of NDVI was mostly controlled by TSW for MNT, while NDVI for MAT was almost equally controlled by TSW and elevation. The improvement of correlations between NDVI and the environmental variables after splitting the data also demonstrated the different spatial patterns of NDVI between MAT and MNT.

Table 2. NDVI regression models in correspondence with Fig. 4. With NDVI indices (EJ-NDVI, GS-NDVI and AP-NDVI) as the dependent variables, single-independent-variable linear or non-linear regressions were run for variables of TSW and elevation. The regressions were performed for: (1) all samples from both transects; (2) splitting samples into two transects; (3) categorizing vegetation types as MAT and MNT.

No.	Fig.	Approach	Model	N	R ²	Sig.
1	4a	EJ-NDVI vs. TSW, all	$Y = 0.0088 e^{0.1034x}$	91	0.7793	**
2	4a	GS-NDVI vs. TSW, all	$Y = 0.0006 x^2 - 0.0196 x + 0.3908$	91	0.7243	**
3	4a	AP-NDVI vs. TSW, all	$Y = 0.0009 x^2 - 0.0313 x + 0.6174$	91	0.6746	**
4	4b	EJ-NDVI vs. Elevation, all	$Y = -1E-06 x^2 + 0.001 x + 0.053$	91	0.7782	**
5	4b	GS-NDVI vs. Elevation, all	$Y = -6E-07 x^2 + 0.0006 x + 0.2665$	91	0.6054	**
6	4b	AP-NDVI vs. Elevation, all	$Y = -4E-07 x^2 + 0.0005 x + 0.3813$	91	0.423	*
7	4c	EJ-NDVI vs. TSW, east	$Y = 0.0171 x - 0.3157$	35	0.8919	**
8	4c	GS-NDVI vs. TSW, east	$Y = 0.0107 x + 0.0256$	35	0.8226	**
9	4c	AP-NDVI vs. TSW, east	$Y = 0.0111 x + 0.1085$	35	0.7586	**
10	4d	EJ-NDVI vs. TSW, west	$Y = 0.0146 e^{0.0904x}$	32	0.8779	**
11	4d	GS-NDVI vs. TSW, west	$Y = 0.0007 x^2 - 0.0228 x + 0.4129$	32	0.8068	**
12	4d	AP-NDVI vs. TSW, west	$Y = 0.001 x^2 - 0.0347x + 0.6413$	32	0.8172	**
13	4e	EJ-NDVI vs. Elevation, east	$Y = -1E-06 x^2 + 0.0011 x - 0.011$	35	0.92	**
14	4e	GS-NDVI vs. Elevation, east	$Y = -8E-07 x^2 + 0.0008 x + 0.2263$	35	0.8769	**
15	4e	AP-NDVI vs. Elevation, east	$Y = -6E-07 x^2 + 0.0007 x + 0.3203$	35	0.834	**
16	4f	EJ-NDVI vs. Elevation, west	$Y = 0.0603 x - 0.0711$	32	0.8821	**
17	4f	GS-NDVI vs. Elevation, west	$Y = 0.0349 x + 0.2022$	32	0.704	**
18	4f	AP-NDVI vs. Elevation, west	$Y = 0.0331 Y + 0.3464$	32	0.5561	**
19		EJ-NDVI vs. TSW, MAT	$Y = 0.0128 e^{0.0971x}$	48	0.8753	**
20		GS-NDVI vs. TSW, MAT	$Y = 0.0006 x^2 - 0.0164 x + 0.3684$	48	0.7586	**
21		AP-NDVI vs. TSW, MAT	$Y = 0.0008 x^2 - 0.0286 x + 0.5992$	48	0.6546	**
22		EJ-NDVI vs. Elevation, MAT	$Y = 0.0578 Y - 0.0649$	48	0.865	**
23		GS-NDVI vs. Elevation, MAT	$Y = 0.0331 Y + 0.2077$	48	0.7254	**
24		AP-NDVI vs. Elevation, MAT	$Y = 0.026 Y + 0.3496$	48	0.5096	**
25		EJ-NDVI vs. TSW, MNT	$Y = 0.0158 x - 0.2862$	43	0.8498	**
26		GS-NDVI vs. TSW, MNT	$Y = 0.0112 x + 0.0115$	43	0.797	**
27		AP-NDVI vs. TSW, MNT	$Y = 0.0128 x + 0.0658$	43	0.729	**
28		EJ-NDVI vs. Elevation, MNT	$Y = -9E-07 x^2 + 0.001 x + 0.0432$	43	0.6678	**
29		GS-NDVI vs. Elevation, MNT	$Y = 0.0326 Y + 0.165$	43	0.5287	**
30		AP-NDVI vs. Elevation, MNT	$Y = 0.0356 \ln x + 0.2508$	43	0.4259	*

**Regression is significant at the 0.01 level (2-tailed); *Regression is significant at the 0.05 level (2-tailed).

Linear and non-linear regression

We used regression models to explore the controls on patterns of NDVI indices (and hence vegetation) along the environmental gradients on both transects. With NDVI indices (EJ-NDVI, GS-NDVI and AP-NDVI) as the dependent variables, single-independent-variable linear or non-linear regressions were run for variables of TSW and elevation. The regressions were performed for: (1) all samples from both transects; (2) MAT on the western transect; (3) MNT on the eastern transect (Table 2).

EJ-NDVI had strong non-linear or linear relations with TSW ($R^2 = 0.779$) and elevation ($r^2 = 0.778$), all

with high significance ($p < 0.01$). Coefficients of determination (r^2) from least squares regression analysis were in the range of 0.605-0.724 for GS-NDVI ($p < 0.01$) and 0.423-0.675 for AP-NDVI ($p < 0.05$). When we grouped the samples into MNT in the eastern transect and MAT in the western transect, more significant regressions were found for both tundra types (Table 2; Fig. 4). In the western transect, all three NDVI indices were found to be significantly related to TSW ($r^2 = 0.807 - 0.878$), but EJ-NDVI had a stronger relation to elevation ($r^2 = 0.882$) than the other two NDVI indices. On the eastern transect, however, all three NDVI indices had a strong correlation to both TSW and elevation. The curves that provide the best fit to these data were quite

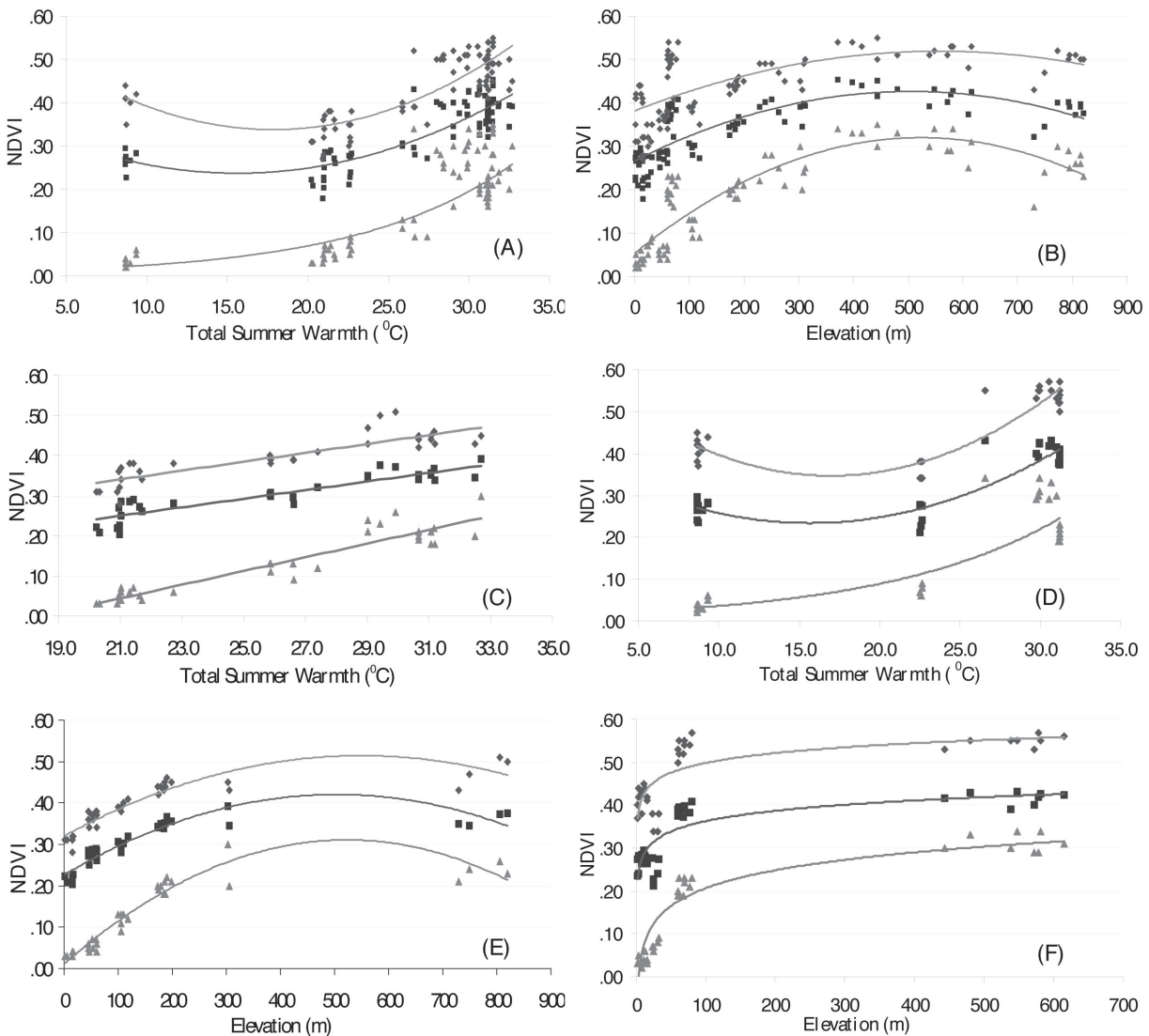


Fig. 4. Scatter plots and trend lines for regression models on NDVI in northern Alaska. **A.** NDVI vs. TSW for all polygons; **B.** NDVI vs. elevation for all polygons; **C.** NDVI vs. TSW for MNT along the eastern transect; **D.** NDVI vs. TSW for MAT along the western transect; **E.** NDVI vs. elevation for MNT along the eastern transect; **F)** NDVI vs. elevation for MAT along the western transect. ◆ = AP-NDVI; ■ = GS-NDVI; triangle = EJ-NDVI. For equations, see regression models in Table 2.

different (Fig. 4): simple linear for NDVI vs. TSW in the east compared to a non-linear in the west; and polynomial for NDVI vs. elevation in the east compared to logarithmic in the west. These reflected the different spatial patterns of both NDVI and environmental factors between the two transects.

Discussion

NDVI values generally followed a latitudinal gradient, i.e. lower values in the north and gradually increasing southwards on both western and eastern transects. EJ-NDVI showed the most significant north-south gradient for both transects. AP-NDVI dropped slightly before reaching the southern end of the transects, due to an increase in elevation. NDVI values showed stronger latitudinal trends, i.e. increased southwards along both gradients of MAT and MNT, especially that of early June and peak values. Strong correlations between early June NDVI and TSW or elevation suggested that this period was most sensitive to the spatial patterns of climate and may be quite sensitive to temporal variability in climate. GS-NDVI and AP-NDVI, both considered as major indices of NDVI and vegetation structure, had less strong correlations with TSW or elevation than EJ-NDVI, although still highly significant ($p < 0.01$). These results indicated that EJ-NDVI was the most sensitive index for spatial environmental variations, and therefore may be a useful variable in spatial modeling in the region.

NDVI was generally controlled by air temperature (i.e. TSW) and elevation. TSW was considered an integrated indicator of growing season air temperatures, while elevation was considered a major contributor to precipitation patterns on the North Slope of Alaska (Haugen & Brown, 1980; Walker et al. 2002). Both TSW and elevation showed significant and strong correlations with NDVI, but TSW was demonstrated to be a more dominant control than elevation. On the western transect, TSW had much greater explanatory power for NDVI patterns than elevation; however, the two variables had almost the same importance on the eastern transect. As many studies suggested, growing season warmth was a dominant factor for plant species composition and vegetation production between physiographic regions in high latitudes (Chapin et al. 1996; Oechel et al. 2000; Arft et al. 1999; Epstein et al. 2000; Billings et al. 1997), and these vegetation-related variables controlled NDVI variables in Arctic tundra ecosystems (Hope et al. 1993; Stow et al. 1993). Moisture regimes may also control patterns of vegetation and thus NDVI on the North Slope (McMichael et al. 1999). Considering its importance to radiation and

water balance, slope could also be one of the major controlling factors on landscape NDVI; further study is clearly needed on this topic to address finer differences in NDVI.

Along the western transect, NDVI indices around the coastal plain (from Barrow to Atkasuk) showed poor response to the gradients of TSW and elevation. In some cases, NDVI in Atkasuk was slightly lower than that in Barrow, located to the north where air temperature is lower (Haugen & Brown 1980). It was suggested that the existence of water bodies in pixels in Atkasuk had contributed to a lower NDVI (Everett 1980). In fact, it is almost impossible to avoid mixed water bodies within any 1.1 km AVHRR pixel in the area (Jia et al. 2000). Also, the spectral brightness at Atkasuk is likely due to its sandy soil substrate, a large component of fruticose lichens and a low shrub biomass (Walker et al. 2002). Another possible contribution is soil brightness; several authors have demonstrated the influence of soil brightness on NDVI (Huete & Jackson 1987). Unlike most of the region, Atkasuk is dominated by sandy soils of almost white colour (Carter 1981; Everett 1980; Walker 1999), which can lead to a higher albedo and thus a lower NDVI (Huete & Jackson 1987).

When the samples for this study were grouped into two tundra types, MAT and MNT, the curves that provide the best fit between NDVI and TSW or elevation were strongly significant. However, when combining all samples from both categories, the significance of correlations declined, and curves also became more non-linear. Costanza & Maxwell (1994) suggested that lowering the resolution of models could increase predictability by averaging out chaotic behaviour at the expense of losing detail about the phenomenon. Our study did not appear to support this argument, however, it was consistent with a finding that, when data were grouped into community types, the curves that provided the best fit between NDVI and environmental variables were linear and quite strong (Shippert et al. 1995). The differences in plant biomass and community composition suggested that MAT and MNT might have very different NDVI-environment relationships. Another recent study also demonstrated a significant difference of intra-seasonal NDVI curves between MAT and MNT, and suggested that this difference should be considered in regional modeling (Jia et al. 2000). Our results supported the ideas that MAT and MNT have different properties and that community type is an appropriate scale for NDVI modeling in tundra.

It has been demonstrated that there is a sharp boundary between MAT and MNT around the Sagwon Hill area on the eastern Alaska transect (Muller et al. 1999;

Walker 1999) and that there were obvious differences in ecosystem properties such as biomass, LAI, and plant species composition between the two sides (MNT to the north and MAT to the south) (Walker et al. 1998; Bockheim et al. 1998). To find out if there is also a significant difference in NDVI at the MAT/MNT boundary, we examined the NDVI and environmental factors for the eight MNT samples located on the north side of the boundary and six MAT samples located on the south side. On the MNT side, EJ-NDVI, GS-NDVI and AP-NDVI were 0.192, 0.342 and 0.456 respectively, compared to the 0.247, 0.390, and 0.502 for the MAT. Because the samples from both sides were quite close to each other, there was unlikely a significant difference in climatic conditions between them, therefore such a gradient should be considered a function of vegetation types.

Both results from the 0.2° latitudinal gradient and NDVI-TSW regression reflected that the vegetation on the Foothills, especially around the transitional zone, was the most sensitive to total summer warmth and most likely to be affected by climate change. These sensitive areas were indicated by the slope/derivative of the spatial functions.

Because MAT and MNT occur on different geologic substrates, it was argued that geology may be one of the major controlling factors of NDVI on the North Slope (Walker et al. 1995, 1999). Walker et al. (1995) concluded in their study that Late Pleistocene glacial surfaces had lower image-NDVI than older Middle Pleistocene surface, and the mean NDVI was correlated with approximate time since deglaciation. They also found that older surfaces had greater cover of shrub-rich tussock tundra and shrub-filled water tracks, and younger surfaces had more dry, well-drained sites with lower biomass and relatively barren non-sorted circles and stripes. Unfortunately we lacked spatial geological data with suitable resolution for our analysis, however our data did support the NDVI differences between potentially younger plant communities (MNT) and older plant communities (MAT).

Due to the sparseness of the measurements used to make the climate map, PRISM data may not well represent the air temperature in some areas, especially in the coastal areas where there is likely much more variation than shown. For example, the map did not portray a steep temperature gradient in the vicinity of Prudhoe Bay. The PRISM data showed apparently warm coastal temperatures around the Prudhoe Bay area compared to Barrow, and no difference between the Prudhoe Bay and Franklin Bluffs to the south, when in fact a doubling of the total summer warmth was observed in field measurements (Walker et al. 2002). Obviously, more detailed examination of the

coastal area climate is needed as further field data become available.

Air temperature and precipitation were normally considered to be two major environmental variables that yield vegetation and NDVI spatial gradients in many regions, even though air temperature was considered more important than precipitation at high latitudes (Brandley et al. 1993; Schmidt & Gitelson 2000). In our study, however, precipitation was excluded from the independent variables for two reasons: first, we do not have enough field precipitation data either to be used directly in modeling or to validate PRISM climate data, and second, precipitation shows a high correlation ($r > 0.91$) with elevation in the region, so we used elevation as a proxy for precipitation. As we have discussed earlier, elevation appeared to be one of the major controlling factors on NDVI in northern Alaska, which may be via the effect of moisture availability on vegetation properties.

In Arctic Alaska, NDVI is likely controlled by TSW and elevation, with the former being dominant. Although our study focused on the spatial heterogeneity of NDVI in related to environmental gradients, it demonstrated the potential usefulness of NDVI in monitoring global change. EJ-NDVI showed the strongest correlation with summer warmth index (TSW), making it likely to be the most sensitive and useful NDVI indicator along environmental gradients in the region.

Acknowledgements. This study was supported by US National Science Foundation project: Arctic Transitions in the Land-Atmosphere System (grant # OPP-9908829). We thank the PRISM program at Oregon State University for providing digital climate maps. We are grateful to Dr. Pep Canadell, R. DeFries, and an anonymous reviewer, for their suggestions and comments on this paper.

References

- Anon. (LAII Science Steering Committee). 1997. *Arctic System Science Land-Atmosphere-Ice Interaction LAII, a plan for action*. University of Alaska, Fairbanks, AK.
- Arft, A.M. et al. 1999. Response patterns of tundra plant species to experimental warming: a meta-analysis of the International Tundra Experiment. *Ecol. Monogr.* 69: 491-511.
- Billings, W.D. 1997. Challenges for the future: Arctic and alpine ecosystems in a changing world. In: Oechel, W.C., Callaghan, T., Gilmanov, T., Holten, J.I., Maxwell, B., Molau, U. & Sveinbjörnsson, B. (eds.) *Global change and arctic terrestrial ecosystems*, pp. 1-20. Springer-Verlag, New York, NY.

- Billings, W.D., Luken, J.O., Mortenson, D.A. & Peterson, K.M. 1982. Arctic tundra: a source or sink for atmospheric carbon dioxide in a changing environment? *Oecologia* 53: 7-11.
- Bockheim, J.G., Walker, D.A., Everett, L.R., Nelson, F.E. & Shiklomanov, N.I. 1998. Soils and cryoturbation in moist nonacidic and acidic tundra in the Kuparuk river basin, arctic Alaska, U.S.A. *Arct. Alp. Res.* 30: 166-174.
- Bradley, R.S., Keiming, F.T. & Diaz, H.F. 1993. Recent changes in the North American Arctic boundary layer in winter. *J. Geophys. Res.* 98: 8851-8858.
- Carter, L.D. 1981. A Pleistocene sand sea on the Alaskan Arctic coastal plain. *Science* 211: 381-383.
- Chapin III, F.S., Shaver, G.R., Giblin, A.E., Nadelhoffer, K.J. & Laundre, J.A. 1995. Responses of Arctic tundra to experimental and observed changes in climate. *Ecology* 76: 694-711.
- Chapin III, F.S., Bret-Harte, M.S., Hobbie, S. & Zhong, H. 1996. Plant functional types as predictors of transient responses of arctic vegetation to global change. *J. Veg. Sci.* 7: 347-358.
- Costanza, R. & Maxwell, T. 1994. Resolution and predictability: an approach to the scaling problem. *Landscape Ecol.* 9: 47-57.
- Epstein, H.E., Walker, M.D., Chapin III, F.S. & Starfield, A.M. 2000. A transient, nutrient-based model of arctic plant community response to climatic warming. *Ecol. Appl.* 10: 824-841.
- Everett, K.R. 1980. Disturbance and variability of soils near Atkasook, Alaska. *Arct. Alp. Res.* 12: 433-446.
- Goward, S.N., Markham, B. & Dye, D.G. 1991. Normalized Difference Vegetation Index measurements from the Advanced Very High Resolution Radiometer. *Remote Sens. Environ.* 35: 257-277.
- Gutman, G., Ignatov, A. & Olson, S. 1994. Towards better quality of AVHRR composite images over land: reduction of cloud contamination. *Remote Sens. Environ.* 50: 134-148
- Hanson, H.C. 1953. Vegetation types in northwestern Alaska and comparisons with communities in other arctic regions. *Ecology* 13: 111-148.
- Haugen, R.K. & Brown, J. 1980. Coastal-inland distributions of summer air temperature and precipitation in northern Alaska. *Arct. Alp. Res.* 12: 403-412.
- Holben, B.N. 1986. Characteristics of maximum-value composite images from temporal AVHRR data. *Int. J. Remote Sens.* 7: 1417-1434
- Hope, A.S., Kimball, J.S. & Stow, D.A. 1993. The relationship between tussock tundra spectral reflectance properties and biomass and vegetation composition. *Int. J. Remote Sens.* 14: 1861-1874.
- Huete, A.R. & Jackson, R.D. 1987. Suitability of spectral indices for evaluating vegetation characteristics on arid rangelands. *Remote Sens. Environ.* 23: 213-232.
- Jia, G.J., Epstein, H.E. & Walker, D.A. 2000. *Spatial and intra-seasonal characteristics of AVHRR-NDVI for the Arctic tundra in Northern Alaska*. Proc. ESA Annual Meeting, Snowbird, UT, pp. 328.
- Markon, C.J. 1999. *Characteristics of the Alaskan 1 km advanced very high resolution radiometer data sets used for analysis of vegetation biophysical properties*. United States Geological Survey, Open File Report 99-088. Anchorage, AK.
- Markon, C.J., Fleming, M.D. & Binnian, E.F. 1995. Characteristics of vegetation phenology over the Alaskan landscape using AVHRR time-series data. *Polar Rec.* 31: 179-190.
- McMichael, C.E., Hope, A.S., Stow, D.A. & Fleming, J.B. 1997. The relation between active layer depth and a spectral vegetation index in arctic tundra landscapes of the North Slope of Alaska. *Int. J. Remote Sens.* 18: 2371-2382.
- McMichael, C.E., Hope, A.S., Stow, D.A., Vourlitis, G., Oechel, W.C. & Fleming, J.B. 1999. Estimating CO₂ exchange at two sites in Arctic tundra ecosystems during the growing season using a spectral vegetation index. *Int. J. Remote Sens.* 20: 683-698.
- Muller, S.V., Racoviteanu, A.E. & Walker, D.A. 1999. Landsat MSS-derived land-cover map of northern Alaska: extrapolation methods and a comparison with photo-interpreted and AVHRR-derived maps. *Int. J. Remote Sens.* 20: 2921-2946.
- Oechel, W.C., Hastings, S.J., Vourlitis, G., Jenkins, M., Riechers, G. & Grulke, N. 1993. Recent change of arctic tundra ecosystems from a net carbon dioxide sink to a source. *Nature* 361: 520-523.
- Oechel, W.C., Vourlitis, G.L., Hastings, S.J., Zulueta, R.C., Hinzman, L. & Kane, D. 2000. Acclimation of ecosystem CO₂ exchange in the Alaskan Arctic in response to decadal climate warming. *Nature* 406: 978-981.
- Shaver, G.R. & Chapin III, F.S. 1991. Production: biomass relationships and element cycling in contrasting arctic vegetation types. *Ecol. Monogr.* 61: 1-31.
- Shaver, G.R., Billings, W.D., Chapin III, F.S., Giblin, A.E., Nadelhoffer, K.J., Oechel, W.C. & Rastetter, E.B. 1992. Global change and the carbon balance in arctic ecosystems. *BioScience* 42: 433-441.
- Shippert, M.M., Walker, D.A., Auerbach, N.A. & Lewis, B.E. 1995. Biomass and leaf-area index maps derived from SPOT images for Toolik Lake and Imnavait Creek areas, Alaska. *Polar Rec.* 31: 147-154.
- Stow, D.A., Burns, B.H. & Hope, A.S. 1993. Spectral, spatial and temporal characteristics of Arctic tundra reflectance. *Int. J. Remote Sens.* 14: 2445-2462.
- Vierling, L.A., Deering, D.W. & Eck, T.E. 1997. Differences in arctic tundra vegetation type and phenology as seen using bidirectional radiometry in the early growing season. *Remote Sens. Environ.* 60: 71-82.
- Viovy, N. 2000. Automatic classification of time series (ACTS): a new clustering method for remote sensing time series. *Int. J. Remote Sens.* 21: 1537-1560.
- Walker, M.D., Walker, D.A. & Auerbach, N.A. 1994. Plant communities of a tussock tundra landscape in the Brooks Range Foothills, Alaska. *J. Veg. Sci.* 5: 843-866.

- Walker, D.A. 1999. An integrated vegetation mapping approach for northern Alaska (1:4 M scale). *Int. J. Remote Sens.* 20: 2895-2920.
- Walker, D.A., Auerbach, N.A. & Shippert, M.M. 1995. NDVI, biomass and landscape evolution of glaciated terrain in northern Alaska. *Polar Rec.* 31: 169-178.
- Walker, D.A. et al. 1998. Energy and trace-gas fluxes across a soil pH boundary in the Arctic. *Nature* 394: 469-472.
- Walker, D.A. et al. In press. Phytomass, LAI, and NDVI in northern Alaska: relationships to summer warmth, soil pH, plant functional types and extrapolation to the circumpolar Arctic. *J. Geophys. Res.*
- Weller, G. et al. 1995. The Arctic Flux Study: a regional view of trace gas release. *J. Biogeogr.* 22: 365-374.

Received 17 January 2001;

Revision received 20 January 2002;

Accepted 28 March 2002.

Coordinating Editor: J. Canadell & P.S. White.